Hindawi Publishing Corporation
Journal of Spectroscopy
Volume 2015, Article ID 832045, 11 pages
http://dx.doi.org/10.1155/2015/832045

Research Article

One and Multiple Bonds Interatomic Spin-Spin Coupling in η^6-Cymene Ru(II) of 3,5-Dimethyl-, 3,5-Dicarboxylic-, and 5-Phenyl-pyrazole Derivatives

Adebayo A. Adeniyi and Peter A. Ajibade

Department of Chemistry, University of Fort Hare, Private Bag X1314, Alice 5700, South Africa

Correspondence should be addressed to Peter A. Ajibade; pajibade@ufh.ac.za

Received 20 September 2015; Revised 7 November 2015; Accepted 15 November 2015

Academic Editor: Artem E. Masunov

The changes in the interatomic distances and the corresponding spin-spin coupling as a result of the hydrolysis of the ruthenium complexes and the effects of different derivatives of the pyrazole ligands and the substituents methyl, carboxylic, and phenyl on the pyrazole rings were studied. A good agreement was obtained between the experimental and the theoretical proton NMR. Significant changes are observed in the isotropic and anisotropic shielding tensor of the atoms and related spin-spin coupling of their bonds due to hydrolysis of the complexes. This observation gives more insight into the known mechanism of activation of the ruthenium complexes by hydrolysis. There are no direct effects of interatomic distances on many of the computed spin-spin couplings with the exception of ^{1}J(Ru-N) which shows significant changes especially within the pair of ^{1}J(Ru-N) in the complexes with two nitrogen atoms of the bis-pyrazole moiety. The magnitude of interatomic spin-spin coupling of the Ru-X follows the order of Ru-Cl > Ru-N > Ru-C > Ru-O. The Ramsey term Fermi contact (FC) has the most significant contribution in most of the computed spin-spin interactions except in ^{1}J(Ru-Cl) and ^{1}J(N-N*) which are predominantly defined by the contribution from the paramagnetic spin orbit (PSO).

1. Introduction

Molecular properties like the spin-spin coupling constant between a pair of atoms in a molecule can give very useful information for analyses of their structure and onset of intramolecular bonding interactions [1, 2]. The spin-spin coupling is an interaction between the magnetic moments of the coupling nuclei. Unlike direct dipolar coupling which is a through-space interaction, the spin-spin coupling is sensitive to bonding interactions and is mediated by the polarization of the spins of the intervening bonding electrons [3]. The classical NMR experiments [4] of the molecules dissolved in liquid crystals [5, 6] are a well-known experimental approach for the determination of the spin-spin interactions but interpretation of the experimental data is often challenging [4]. Through the computational method, the interpretation of the spin-spin coupling is much easier by partition of the spin-spin property into contributing Ramsey terms [7] which are made up of the Fermi contact (FC), spin dipole (SD), diamagnetic spin orbit (DSO), and paramagnetic spin orbit (PSO) [8].

The general expectation is that there should be diminishing in the values of the coupling interactions as the number of bonds between two nuclei increases [1, 2]. However, it is possible to obtain large coupling constants even when coupling atoms are many bonds apart as far as there is close proximity between the two nuclei. In this research six η^6-cymene ruthenium complexes of pyrazole derivatives (Figure 1) which have methyl, carboxylic, and phenyl group on C3 and C5 were synthesised and their proton NMR spectra were related to the theoretical modelling. The effects of hydrolysis on the NMR and intramolecular spin-spin interactions in the mono- and bidentate derivatives of pyrazole complexes were considered.

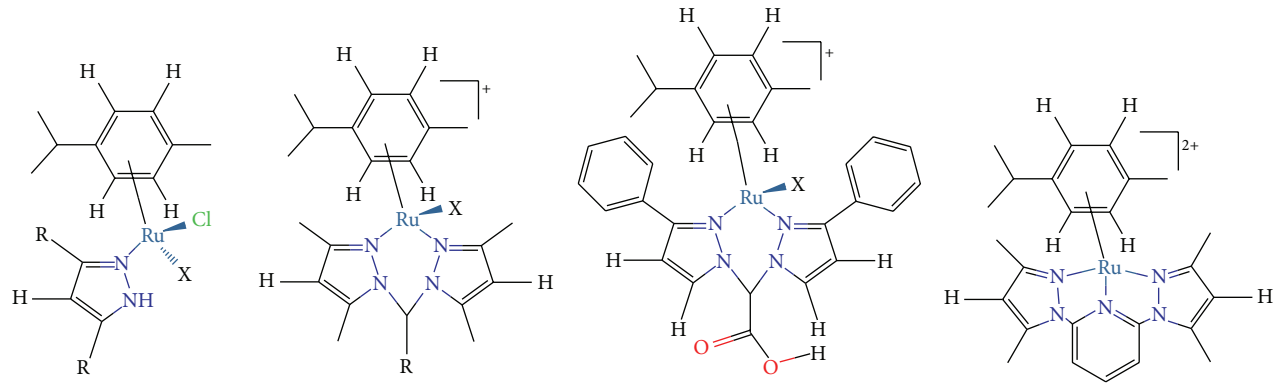

(**1a**) R = CH_3, X = Cl
(**1b**) R = CH_3, X = H_2O
(**2a**) R = COOH, X = Cl
(**2b**) R = COOH, X = H_2O

(**3a**) R = H, X = Cl
(**3b**) R = H, X = H_2O
(**4a**) R = COOH, X = Cl
(**4b**) R = COOH, X = H_2O

(**5a**) X = Cl
(**5b**) X = H_2O

(**6**)

Figure 1: The molecular representation of η^6-cymene (Cym) ruthenium(II) derivatives of 3,5-dimethylpyrazole (**1a**), 3,5-diaceticpyrazole (**2a**), bis(3,5-dimethylpyrazol-1-yl)methane (**3a**), bis(3,5-dimethylpyrazol-1-yl)acetic (**4a**), bis(5-phenylpyrazol-1-yl)acetic (**5a**), and bis(3,5-dimethylpyrazol-1-yl)pyridine (**6**) complexes with their hydrated forms. The explicit hydrogen atoms shown are of interest.

This makes the total number of theoretical molecules added up to eleven complexes. Hydrolysis is known to be an important process which defines the activation of metal complexes in their biological application as anticancer drugs [9–12].

Some of the research interests are to know the extent of the effects of pyrazole unit substituents and the types of the pyrazole ligand (mono-, bi-, and tridentate) on the ruthenium-ligand spin-spin coupling and also on the $^3J(H\cdots H)$ spin-spin coupling of the four hydrogen atoms (4H) of the benzene ring of the cymene ligand in the complexes. Also of interest is the change in the intramolecular spin-spin interactions in the complexes as a result of hydrolysis which is well defined mechanism for the activation of the metal complexes in anticancer application.

2. The Computational and Experimental Methods

2.1. Computational Details. All the calculations were accomplished using the Gaussian 09 (G09) version D01 [13]. The optimized geometries of the eleven derivatives of η^6-cymene Ru(II) complexes were obtained using PBE exchange functional [14, 15] and no negative harmonic force constants were obtained in all the complexes as a clear indication that local minimums were obtained. During the optimization, all atoms in each of the complex were treated with 6-31+G(d,p) [16–18] except Ru atom which was treated with basis set SBKJC VDZ [19] (obtained from EMSL Basis Set Library [20, 21]) and a total of 28 core electrons were removed from Ru (1s, 2s, 2p, 3s, 3p, and 3d) atom. The basis set SBKJC VDZ comes with effective core potential and has been applied in computing properties of many metal clusters [22, 23]. DFT PBE exchange functional has been found to be good for the optimization of metal complexes and give similar results with hybrid functional PBE0 and mPW1PW91 [24]. It is also good for studying weak-interacting systems [25] but just like any other DFT methods, it is limited in the study of noncovalent intermolecular interactions because of its long-range deficiency which makes hybrid DFT preferable [26–28]. Even though all the properties of interest are purely intramolecular interaction, the NMR, spin-spin coupling constants J(A, B) [29, 30], and other stationary properties were computed using B3LYP hybrid DFT method which is Becke's three-parameter exchange [31] and Lee-Yang-Parr's correlation nonlocal functional. In the stationary phase computation of NMR and their spin-spin interactions, all electron basis set DGDZVP [32, 33] was used for Ru atom while other atoms were still treated with 6-31+G(d,p) as in optimization step. The Gauge-Independent Atomic Orbital (GIAO) method was used to compute the NMR properties. The direct and fitting methods were used for the calculation of the theoretical ^{1}H-NMR chemical shift. In direct method, the isotropic shielding of each proton in the complexes was directly subtracted from that of the reference tetramethylsilane (TMS) while in fitting method the reported equation $\sigma^1H = 31.0 - 0.97 * \sigma^1H$ in the literature [34] was applied.

2.2. Experimental Synthesis of the Complexes. The first step is the synthesis of the precursor $[(cym)RuCl_2]_2$ by reacting $RuCl_3{\cdot}3H_2O$ with 8.0 equivalent mmol of p-phellandrene in ethanol. A similar approach as was reported in a literature was adopted [35] only that 8.0 mmol equivalent of p-phellandrene was used instead of approximately 10 mmol equivalent. All the complexes are then obtained from the precursor $[\eta^6$-$(cym)RuCl_2]_2$ interaction with 2.2 equivalent of each ligand and reflux for 6–12 h. The synthesis of the complexes follows a similar method used for the synthesis of RAPTA complexes [36, 37].

3. Result and Discussion

3.1. The Geometries Properties. Six η^6-cymene ruthenium complexes dmpzRu(II)Cym (**1a**), dcpzRu(II)Cym (**2a**), bdmpzmRu(II)Cym (**3a**), bdmpzaRu(II)Cym (**4a**), bphpzaRu(II)Cym (**5a**), and bdmpzpyRu(II)Cym (**6**) (Figure 1) were synthesised and their proton NMR property was determined. All the six synthesised complexes and their respective hydrated form dmpzRu(II)WCym (**1b**), dcpzRu(II)WCym (**2b**), bdmpzmRu(II)WCym (**3b**), bdmpzaRu(II)WCym (**4b**), and bphpzaRu(II)WCym (**5b**) with tridentate derivatives **6** were studied computationally. The peculiar features which are of interest in this research are the effect of the methyl, carboxylic, phenyl group, and hydrolysis on their NMR and spin-spin coupling.

The bond distances which define all the spin-spin coupling of interest in the complexes are shown in Table 1 and selected bond angles are shown in Table 2. The spin-spin couplings which are of interest are those which involved the one-bond distance coupling of ruthenium-ligand bonds (^{1}J(Ru-X) where X stands for C, Cl, N, and O), three-bond distance (^{3}J(Hc$\cdots$Hc)) of the 4H atoms of the benzene ring of cymene ligand, the four-bond distance coupling of the two coordinating nitrogen atoms of the bidentate ligands ^{4}J(N$\cdots$N), three- and six-bond distance coupling of three coordinating nitrogen atoms of the tridentate ((^{3}J(N$\cdots$Np)) and ^{6}J(N$\cdots$N) where Np stands for the coordinating nitrogen atom of the pyridine unit), one-bond ^{1}J(C-H) coupling of the C4-H in pyrazole unit, and the three-bond distance hydrogen atoms of the pyrazole unit in the ligand **5a** (^{3}J(H$\cdots$H)). There is gradual decrease in the N$\cdots$N interatomic distance of complexes with bidentate as a result of hydrolysis which should be direct effect of their decrease in N-Ru-N bond angle (Table 2). The bond distances of N-H decrease also upon hydrolysis while C-H bond distances are relatively the same in all the complexes. All the metal-ligand bonds (Ru-X) follow the order of Ru-Cl > Ru-C, Ru-O > Ru-N.

It is interesting to point out the relationship in the properties of the pair of Ru-N bonds in the bis-pyrazole derivatives of the complexes. The bidentate and tridentate derivatives show a very little difference between bond distances of the pair of Ru-N ranges from 0.01 Å in **3a** and its hydrated form **3b** to 0.03 Å in complex **4b** (Table 1). The differences in the pair of Ru-N bonds' distances are not the direct effect of their monodentate ligand Cl or H_2O position since the Cl atom in **4a** forms almost the same angle with the two coordinating N atoms (having N-Ru-Cl bond angles of 84.52° and 84.13° as shown in Table 2) and yet has the highest variation in the pair of its Ru-N bonds compared to other complexes that have higher bond differences with their monodentate ligand Cl or H_2O.

3.2. The ^{1}H-NMR, Isotropic, and Anisotropic Shielding Tensor. The experimental ^{1}H-NMR spectra of the complexes **3a**, **5a,** and **6** derivatives are shown in Figure 2 and the comparison of all the synthesised experimental shifts with the theoretical direct and fitting methods is shown in Table 3. The unique feature in complex **3a** which is absent in the **5a** and **6e** is

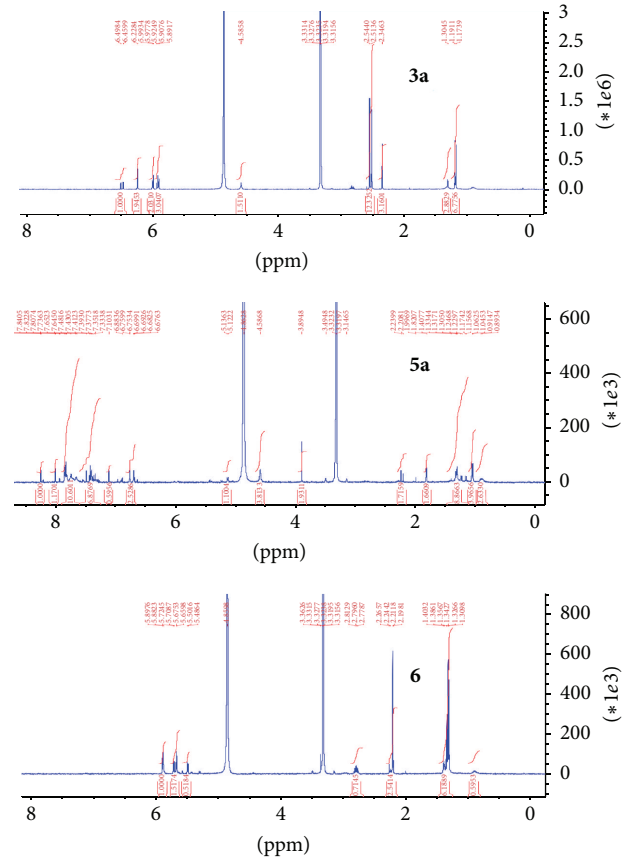

Figure 2: The experimental proton NMR of the complexes **3a**, **5a,** and **6** derivatives obtained in the CD_3OD solvent.

the proton shift of the pyrazole linking CH_2 which shows a long singlet peak around −3.8948 (Figure 2). The pyridine unit in **6** makes the span of its hydrogen shift higher than **3a** and the two phenyl units in the complex **5a** result in a much more wider shift of its proton atoms. There is a good agreement between the experimental and the theoretical ^{1}H-NMR especially for the CH_3 substituent (Table 3). The methyl protons which are pointing towards the Ru atom are very low in shift while those pointing towards the chloride ion are higher in chemical shifts. It is only in complex **6** that proton shift of C4-H of the pyrazole unit spans a wider range theoretically compared to their experimental range.

There is a significant increase in the magnitude of both isotropic and anisotropic shielding tensor of ruthenium atom due to hydrolysis. This can serve as one of the indicators for the activation process of the metal complexes in their anticancer application. Likewise, the shielding of the coordinating nitrogen atoms and their anisotropic tensor increases significantly upon hydrolysis. In all of the selected atoms in Table 4, the magnitudes of the isotropic shielding tensor of the atoms are lower than their corresponding anisotropic shielding tensors except for the Cl atoms. The isotropic shielding tensor of the coordinating nitrogen atoms (N) is lower than that of the other nitrogen atoms (N*) which are not involved in coordination while their anisotropic tensors are reverse of the isotropic tensor. It is only in the complex **2a** that the

Table 1: Selected interatomic bond distances of interest in Angstroms.

	1a	1b	2a	2b	3a	3b	4a	4b	5a	5b	6
Ru-C	2.23	2.27	2.18	2.19	2.23	2.26	2.22	2.26	2.23	2.21	2.25
Ru-C	2.20	2.18	2.18	2.28	2.31	2.31	2.31	2.21	2.30	2.28	2.26
Ru-C	2.21	2.24	2.25	2.19	2.20	2.25	2.20	2.26	2.24	2.21	2.30
Ru-C	2.20	2.18	2.25	2.22	2.25	2.21	2.26	2.22	2.28	2.24	2.31
Ru-C	2.22	2.21	2.21	2.26	2.28	2.20	2.29	2.24	2.20	2.31	2.23
Ru-C	2.24	2.26	2.24	2.20	2.21	2.25	2.21	2.30	2.20	2.24	2.24
Ru-N	2.15	2.14	2.23	2.15	2.15	2.15	2.16	2.18	2.17	2.17	2.15
Ru-N/Ru-Cl	2.42	2.42	2.47	2.41	2.16	2.14	2.19	2.16	2.19	2.17	2.16
Ru-Cl/O/Np	2.46	2.24	2.42	2.27	2.41	2.24	2.40	2.23	2.41	2.19	2.07
Hc$\cdots$Hc	2.49	2.49	2.49	2.47	2.50	2.50	2.50	2.50	2.49	2.51	2.49
Hc$\cdots$Hc	2.49	2.51	2.47	2.50	2.50	2.50	2.50	2.50	2.49	2.50	2.51
C-H	1.09	1.09	1.09	1.09	1.09	1.09	1.09	1.09	1.09	1.09	1.09
C-H					1.09	1.09	1.09	1.09	1.09	1.09	1.09
N-N	1.36	1.36	1.33	1.35	1.37	1.38	1.39	1.39	1.37	1.38	1.41
N-N					1.37	1.38	1.38	1.39	1.37	1.37	1.41
Nz$\cdots$Nz					2.95	2.92	3.00	2.95	3.06	2.86	3.40
Nz$\cdots$Np									2.77	2.77	2.49
Nz$\cdots$Np									2.77	2.77	2.48
N-H	1.04	1.02	1.05	1.02							

Table 2: Selected bond angles of interest in the complexes.

	1a	1b	2a	2b	3a	3b	4a	4b	5a	5b	6
N-Ru-N					86.32	85.77	87.33	85.83	88.90	82.31	104.25
N-Ru-Cl/O	84.04	85.34	85.02	86.30	84.18	82.05	84.52	83.51	82.15	86.56	71.86
N-Ru-Cl/O	85.77	80.47	81.47	87.34	84.57	80.40	84.13	80.77	83.76	86.90	72.20
Cl-Ru-Cl/O	89.09	76.14	87.45	75.66							

coordinating nitrogen is found to be deshielded (negative isotropic value) due to the presence of two carboxylic groups on the pyrazole unit. The isotropic shielding and anisotropic tensors of Hc atoms of cymene are little higher than Hz atoms of the pyrazole. The isotropic shielding of Hc atoms is within a very close range in all the complexes but their anisotropic tensors are found higher in the complexes with monodentate pyrazole units. In the complexes with monodentate pyrazole unit, the anisotropic properties of the Hn atoms significantly reduce upon hydrolysis while there is a slight increase in their isotropic shielding tensors.

3.3. The Spin-Spin Coupling Interaction. The graphical representation of selected spin-spin interactions in the complexes is shown in Figure 3 and the details of all their spin-spin are shown in Table 5. In many of the experimental characterisations of derivatives of η^6-cymene Ru(II) complexes, the values of the spin-spin ^{3}J(Hc$\cdots$Hc) of benzene ring are often presented as part of their characterisation and have been reported in the literature to have experimental ranges of 6–8 [38, 39], 6 [40, 41], 5.7–6.2 [42], 6.4 [43], and 6.02–6.56 [44] which agree with our computed ranges of 6.124 in **1a** to 7.151 in **6**. The changes in the spin-spin coupling of the complexes as corresponding effect of the type of the monodentate, bidentate, and tridentate ligands and hydrolysis of the complexes are examined. All the spin-spin couplings of ^{1}J(Ru-C), ^{1}J(Ru-Cl), ^{1}J(Ru-N), ^{1}(N-N), ^{3}J(N$\cdots$Np), and ^{n}J(N$\cdots$N) are negative in values while ^{1}J(Ru-O), ^{1}J(C-H), ^{3}J(Hc$\cdots$Hc), and ^{3}J(H$\cdots$H) are positive. The conventional signs of the coupling do not directly follow the proposed convection of positive for one-bond coupling constants, negative for two-bond coupling constants, and positive for three-bond coupling constants based on the generalized Dirac vector mode [4]. It is expected that as the number of bonds between the two nuclei increases their coupling should diminish [1, 2]. The magnitude of interatomic spin-spin coupling of the Ru-X follows the order of Ru-Cl > Ru-N > Ru-C > Ru-O which does not correspond to the expected reverse of their corresponding interatomic bond distances. The possible explanation for the higher spin-spin coupling of Ru-Cl above other Ru bonds in the compounds is the predominant HOMO feature of the Cl atom in the complexes as shown in Figure 4. It would also be expected that values of the coupling interaction of the ^{1}J(N-N) are higher than all other spin-spin couplings because of its lower bond distance except for the ^{1}J(C-H) and ^{1}J(N-H) (Table 1), but its values

Table 3: The experimental and the theoretical (direct and fitting) of the ^{1}H-NMR of the complexes in ppm.

	Direct	Fitting	Experimental
		1a	
CH_3	0.94 to 3.05	1.44 to 3.48	1.33 to 2.50
C-Hc	3.45	3.87	2.86
C4-H	5.921	6.27	6.06
C_{others}-H	4.64 to 5.13	5.02 to 5.50	5.49 to 6.28
NH	12.35	12.50	6.18
		2a	
CH_3	0.79 to 2.99	1.29 to 3.42	0.31 to 2.62
C-Hc	3.44	3.86	2.84
COOH	6.09, 6.30	6.431, 6.64	6.49
C_{others}-H	5.18 to 6.09	5.55 to 6.43	5.25 to 8.10
C4-H	7.47	7.77	
NH	14.12	14.22	
		3a	
CH_3	1.15 to 3.4373	1.63 to 3.86	1.19 to 2.5
C-Hc	3.58	3.99	2.85
C_{others}-H	5.13 to 5.28	5.50 to 5.64	4.59 to 5.99
CH_2	5.49, 5.55	5.84, 5.91	6.22
C4-H	6.26, 6.27	6.59, 6.60	6.46, 6.50
		4a	
CH_3	1.06 to 3.48	1.55 to 3.90	1.25 to 2.55
C-Hc	3.71	4.13	2.80
C4-H	6.18, 6.33	6.52, 6.66	6.18
C_{others}-H	5.12 to 6.33	5.49 to 6.66	5.25 to 6.25
COOH	7.00	7.31	7.2
CHOO	8.14	8.41	8.15
		5a	
CH_3	0.12 to 2.67	0.64 to 3.11	0.89 to 4.59
C-Hc	2.86	3.30	2.24
CHOO	6.61	6.94	6.88
COOH	7.35	7.65	7.74
C4-H	6.48, 6.52	6.81, 6.84	6.76
C_{others}-H	3.96 to 8.17	4.36 to 8.45	3.89 to 8.24
		6	
CH_3	0.36 to 3.20	0.87 to 3.63	0.85 to 2.27
C-Hc	2.02	2.49	2.80
C4-H	4.99 to 8.40	5.37 to 8.67	5.50 to 5.90
C_{others}-H	6.75, 6.91	7.07, 7.22	5.71, 5.72

are lower than many of the other interatomic couplings with longer bond distances. In addition, since there is a gradual decrease in N⋯N interatomic distances upon hydrolysis of complexes with bidentate nitrogen chelating ligands (Table 1), one would expect the spin-spin interaction of ^{3}J(N⋯N) in hydrated complexes to be higher but the reverse is the case (Table 5). Also, the bond distances of N⋯Np (Table 1) are shorter than many of the N⋯N bond distances but its spin-spin coupling values are lower than many of the spin-spin values of the N⋯N (Table 5). The coupling and FC of some intramolecular atoms of molecules have been found to be

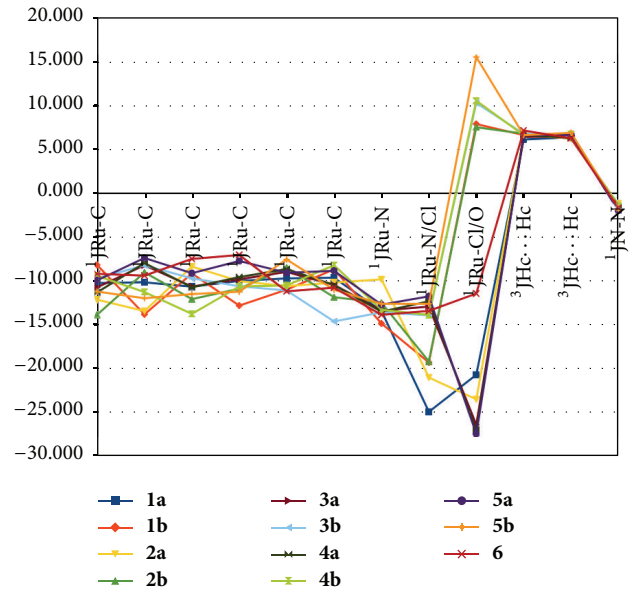

Figure 3: Features of changes in the selected spin-spin coupling of ruthenium(II) η^6-cymene complexes of dimethylpyrazole derivatives and their hydrated forms.

independent of the bond types and distances [4] unlike the coupling of intermolecular hydrogen bonding. The reason has been traced to the consequence of the absence of an explicit distance-dependent term in the FC operator [4]. It is possible to obtain large coupling constants even when lying many bonds apart as far as there is close proximity between two nuclei.

The little differences in the Ru-N bond distances affect their pair of spin-spin couplings ^{1}J(Ru-N) as the complexes **4a** and **5a** which have a bond differences of 0.03 and 0.02 Å in their pair of Ru-N also have the highest differences between their pair of spin-spin couplings, 1.188 and 0.944, respectively, compared to other complexes (Table 5). Out of all the ^{1}J(Ru-O) of the hydrated complexes, **5b** has the highest magnitude while **2b** has the lowest (Figure 3 and Table 5) which is inversely proportional to their bond distances (Table 1). All the ^{1}J(Ru-C) span the range of −7.033 in **6** to −14.610 in **3b**. The magnitude of spin-spin interaction ^{1}J(Ru-Cl) is lower in monodentate compared to bidentate complexes and even much lower after hydrolysis (Figure 3). There is significant increase in the magnitude of ^{1}J(C-H) and ^{1}J(N-H) upon hydrolysis. The coupling of ^{1}J(N-N) decreases slightly upon hydrolysis (except for its increased hydrolysed complex **2b** compared to its nonhydrolysed form **2a**) and its values range from −1.293 in the complex **2a** to −2.043 in complex **5a**.

3.4. Ramsey Terms and Their Correlation with Spin-Spin Interatomic Interaction. The Ramsey terms SD, FC, PSO, and DSO which defined each of the spin-spin coupling interactions for the selected interatomic distances of interest in the complexes are presented in Supplementary Table S1 (see Supplementary Material available online at http://dx.doi.org/10.1155/2015/832045). The most significant

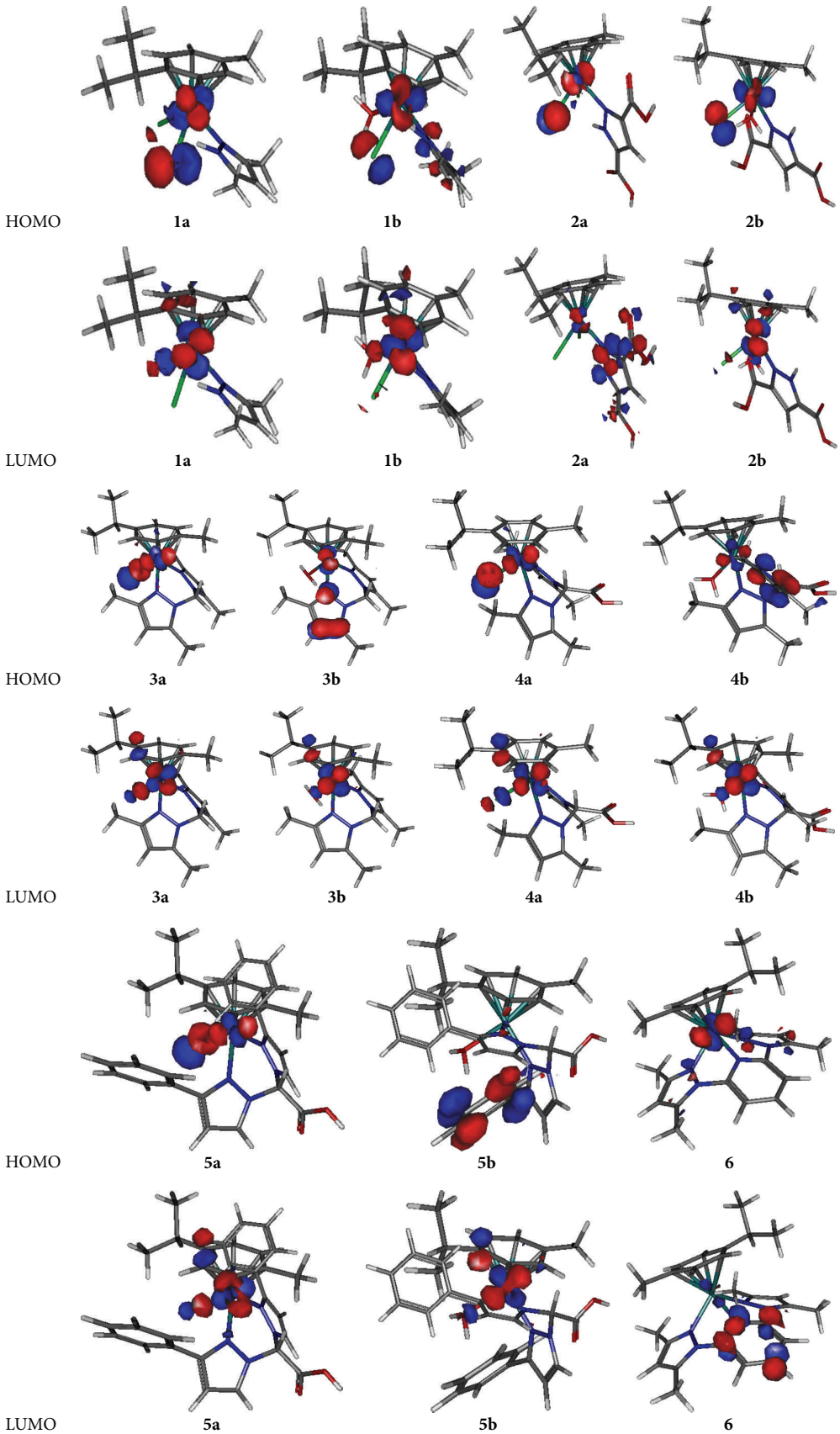

Figure 4: The HOMO and the LUMO features of the compounds constructed with isovalue of 0.07.

Table 4: The isotropic and anisotropic shielding tensor of selected atoms of interest in the complexes.

	1a	**1b**	**2a**	**2b**	**3a**	**3b**	**4a**	**4b**	**5a**	**5b**	**6**
						Isotropic					
Ru	−3579.05	−4052.62	−3779.82	−4329.67	−3878.80	−4817.44	−3990.26	−4956.22	−4157.77	−5180.49	−4198.88
C	84.02	72.18	97.57	119.09	113.37	113.63	112.19	114.26	115.81	95.32	94.34
Cl/O/Np	1092.32	345.21	1056.76	347.52	1090.80	362.02	1071.29	364.57	1041.85	385.12	55.17
N	15.41	37.09	−25.88	−6.79	23.40	41.88	13.14	35.95	14.61	29.47	8.15
N*	50.81	69.66	20.66	52.98	53.51	55.49	52.16	51.46	49.17	48.07	28.49
Hc	26.78	26.11	25.96	25.95	26.22	25.38	26.13	25.51	26.41	26.12	25.05
Hz	25.50	25.07	23.94	23.91	25.15	24.70	25.24	24.71	24.94	24.53	24.67
C4	85.80	83.35	76.86	79.73	81.46	78.99	80.33	79.24	80.20	79.38	77.79
Hn	19.07	22.60	17.29	21.13							
Cl	1103.90	993.23	1043.74	950.90							
						Anisotropic					
Ru	6354.73	6985.62	6498.56	7253.65	6037.92	7308.65	6076.09	7374.64	6342.14	7391.59	6402.18
C	142.17	158.38	115.22	120.69	111.24	126.25	111.68	126.21	114.64	113.19	119.93
Cl/O/Np	378.43	117.72	290.77	155.04	350.71	113.78	355.15	110.23	441.50	264.39	224.00
N	218.70	162.05	324.97	263.88	165.09	134.85	127.97	119.33	177.02	151.81	100.63
N*	133.67	95.86	196.55	112.14	101.69	98.38	97.43	98.05	114.64	114.75	77.13
Hc	6.21	6.13	6.45	6.09	4.97	4.10	4.42	4.33	5.45	6.98	3.08
Hz	4.06	4.10	5.36	4.87	3.91	4.23	3.86	4.40	5.20	4.59	4.32
C4	89.45	100.23	127.83	132.19	91.93	97.33	89.69	102.12	113.69	117.32	99.46
Hn	21.10	8.88	22.25	7.07							
Cl	438.67	429.75	269.22	521.67							

Table 5: Selected spin-spin coupling of the complexes.

	1a	**1b**	**2a**	**2b**	**3a**	**3b**	**4a**	**4b**	**5a**	**5b**	**6**
^{1}JRu-C	−10.229	−8.180	−12.133	−13.854	−10.728	−9.717	−11.302	−9.409	−9.927	−11.207	−9.185
^{1}JRu-C	−10.152	−13.808	−13.433	−9.019	−8.204	−8.213	−7.953	−11.260	−7.377	−11.968	−9.390
^{1}JRu-C	−10.647	−9.147	−8.353	−12.067	−10.632	−9.697	−10.725	−13.750	−9.110	−11.491	−7.483
^{1}JRu-C	−9.995	−12.805	−10.014	−10.880	−9.809	−10.600	−9.557	−10.626	−7.721	−11.220	−7.033
^{1}JRu-C	−9.705	−10.989	−10.590	−8.483	−8.967	−11.085	−8.637	−10.505	−9.061	−7.547	−11.181
^{1}JRu-C	−9.630	−8.671	−10.181	−11.846	−10.443	−14.610	−10.472	−8.208	−8.844	−10.995	−10.765
^{1}JRu-N	−13.418	−14.851	−9.813	−12.478	−13.370	−13.577	−13.501	−13.279	−12.698	−12.607	−13.862
^{1}JRu-N/Cl	−24.916	−19.288	−21.008	−19.173	−12.917	−13.921	−12.313	−13.869	−11.754	−12.599	−13.410
^{1}JRu-Cl/O	−20.695	7.894	−23.491	7.530	−26.381	10.290	−26.967	10.540	−27.442	15.530	−11.433
^{3}JHc···Hc	6.124	6.631	6.663	6.795	6.406	6.780	6.647	6.624	6.610	6.631	7.151
^{3}JHc···Hc	6.385	6.245	6.259	6.370	6.527	6.532	6.295	6.727	6.627	6.895	6.269
^{1}JN-N	−1.443	−1.436	−1.293	−1.366	−1.649	−1.480	−1.579	−1.558	−2.043	−1.778	−1.670
^{1}JN-N					−1.602	−1.444	−1.779	−1.379	−2.167	−1.759	−1.783
^{n}JN···N					−0.425	−0.385	−0.338	−0.284	−0.373	−0.343	−0.068
^{1}JC-H	182.811	188.593	196.667	202.375	188.943	193.705	188.268	193.111	188.285	199.320	192.338
^{1}JC-H					188.932	193.874	190.010	193.288	188.134	199.256	195.214
^{n}JN···Np/^{3}JH···H									2.885	3.023	−0.324
^{n}JN···Np/^{3}JH···H									2.895	3.016	−0.363

Ramsey term that contributes mostly to the spin-spin interactions is FC except for the Ru-Cl and N-N* which are predominantly defined by the contribution from the PSO. Also, PSO contribution to the Ru-O spin-spin interaction is higher than FC in complexes with monodentate pyrazole derivatives. The properties of the Ramsey terms for the Ru-Cl are very unique; after the most significant contribution from the PSO, there is also a significant contribution from SD which in complexes like **3a** and **4a** is higher than the contribution from the FC. Also, PSO is the most significant

Table 6: The correlations between the Ramsey terms, spin-spin coupling, and isotropic and anisotropic shielding and their interatomic distance.

	FC	SD	PSO	DSO	J-Coup	Dist
FC	1.00	0.28	0.17	0.59	1.00	−0.69
SD	0.28	1.00	0.87	0.28	0.35	−0.25
PSO	0.17	0.87	1.00	0.20	0.24	−0.19
DSO	0.59	0.28	0.20	1.00	0.60	−0.26
J-Coup	1.00	0.35	0.24	0.60	1.00	−0.70
Dist	−0.69	−0.25	−0.19	−0.26	−0.70	1.00
Iso1	0.48	0.25	0.27	0.63	0.50	−0.35
Aniso1	−0.48	−0.27	−0.29	−0.64	−0.50	0.34
Iso2	−0.14	−0.77	−0.89	−0.21	−0.21	0.19
Aniso2	−0.44	−0.65	−0.67	−0.60	−0.49	0.28
Ave(Iso)	0.48	0.18	0.18	0.62	0.49	−0.34
Ave(Aniso)	−0.48	−0.28	−0.30	−0.64	−0.50	0.34

Ramsey term in all the N-N* spin-spin followed by the contribution of FC except for the complexes **4a**, **5a,** and **6** where FC contribution is higher than the PSO. The entire Ru-C and Ru-N spin-spin coupling are defined mostly by the contribution from their FC followed by small contribution of the PSO but the PSO contribution improves slightly upon hydrolysis. Also FC is the most significant Ramsey term which defines all H···H, C-H, and N-H spin-spin coupling but next contributing Ramsey terms is their DSO.

The correlation (R^2) and the linear equation of the Ramsey terms, the interatomic distances, and isotropic and anisotropic tensors of the two atoms involved in the spin-spin coupling and their respective sum are shown in Figure 5 while the correlations within all the terms are shown in Table 6. Just as the FC is found to be the most significant Ramsey terms that define many of the interatomic spin-spin interactions in the complexes, the trend of changes in its values is also found to be highly correlated ($R^2 = 0.99$) with the trend of changes in all the spin-spin interactions of the complexes (Figure 5). Even though in many of the interactions of interest the PSO contribution is significant yet it has a very poor correlation ($R^2 = 0.06$) with the trend of changes in the spin-spin interaction that is poorer than the SD term ($R^2 = 0.12$) which has a very negligible contribution to most of the spin-spin interactions. The correlation of DSO ($R^2 = 0.37$) with the trend of changes in the spin-spin coupling is relatively better followed by the correlation of their respective interatomic distances ($R^2 = 0.34$). As shown in Table 6, there is significant and inverse correlation between the interatomic distances and their FC and spin-spin interaction. There is significant correlation between the SD and PSO and also between the FC and DSO. The Iso1 and Aniso1 which are predominantly from the ruthenium atoms are significantly correlated with the DSO while the Iso2 and Aniso2 are significantly correlated with the SD and PSO. The averages of the isotropic and anisotropic of the two atoms involved in the spin-spin coupling are significantly correlated mostly with the DSO.

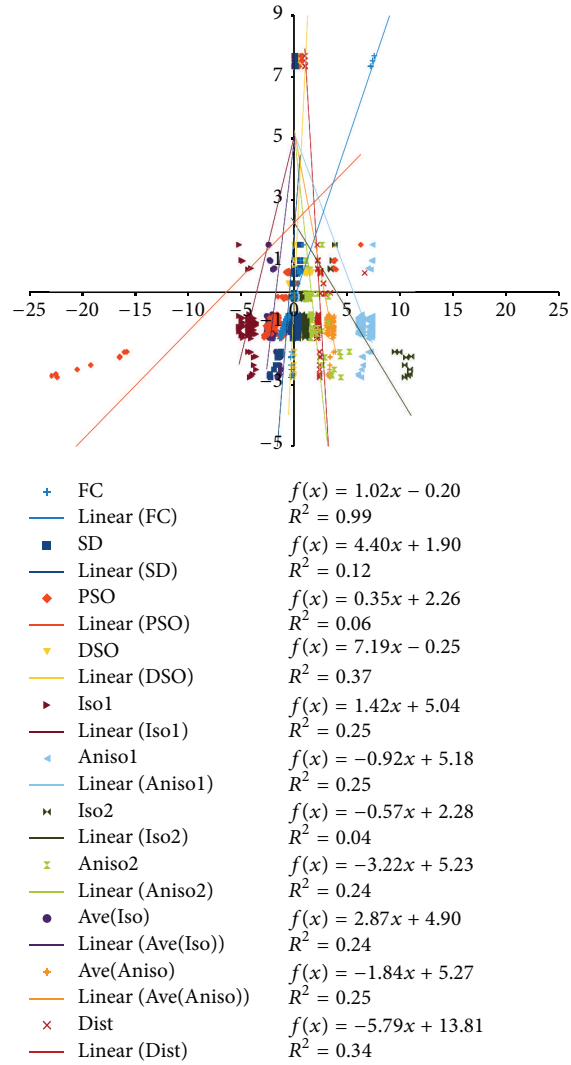

Figure 5: The linear equation and the correlation (R^2) of J-coupling of selected atoms with their Ramsey terms, isotropic, anisotropic, average isotropic, and anisotropic shielding tensor of the two atoms involve spin-spin coupling. The suffixes 1 and 2 of the Iso and Aniso indicate first and second atom that are involved in the coupling. The J-coupling and FC were scaled with 0.1; Iso1, Aniso1, Ave(Iso), and Ave(Aniso) were scaled by 0.001 while Iso2 and Aniso2 were scaled by 0.01 in the plot.

4. Conclusion

The experimental and the theoretical proton ^{1}H-NMR of η^6-cymene Ru(II) complexes with monodentate, bidentate, and tridentate of pyrazole derivatives were studied and a very good agreement was obtained between the experimental and theoretical methods. The features and the relations between the geometrical interatomic distances, angles, and the spin-spin coupling which involve all the Ru-ligand bonds and one bond or many bonds' interaction of interest as results of the nature of the substituents and the ligands were presented. Through the theoretical modelling, the very low proton shifts in the experimental results are found to be the methyl protons which are pointing towards the Ru atom while those pointing

towards the chloride ion have higher chemical shifts. A gradual decrease in the N⋯N interatomic distance of complexes was observed in the bidentate derivatives as a result of hydrolysis which is a direct effect of the decrease in the N-Ru-N bond angle of the hydrolysed complexes compared to the nonhydrolysed ones. There is a significant increase in the magnitude of both isotropic and anisotropic shielding tensor of ruthenium atom due to hydrolysis. The anisotropic properties of the Hn atoms of complexes with monodentate pyrazole unit significantly reduce upon hydrolysis while their isotropic shielding tensors slightly increased. Likewise, the shielding of the coordinating nitrogen atoms and their anisotropic tensor increases significantly upon hydrolysis. The changes in the anisotropic and isotropic tensors of the complexes upon hydrolysis can serve as a good parameter to define the mechanism of their activation by hydrolysis which is important for their application as anticancer. The computed spin-spin coupling of the benzene ring of the cymene unit of the complexes is within the experimental ranges that have been reported for similar complexes. All the spin-spin couplings of ^{1}J(Ru-C), ^{1}J(Ru-Cl), ^{1}J(Ru-N), ^{1}(N-N), ^{3}J(N⋯Np), and ^{n}J(N⋯N) are negative in values while ^{1}J(Ru-O), ^{1}J(C-H), ^{3}J(Hc⋯Hc), and ^{3}J(H⋯H) are positive. In many of the computed spin-spin couplings, there is no direct relation between their interatomic distances and their spin-spin couplings. The magnitude of interatomic spin-spin coupling of the Ru-X follows the order of Ru-Cl > Ru-N > Ru-C > Ru-O which does not correspond to the expected reverse of their corresponding interatomic bond distances. The little difference between bonds distances of the pair of Ru-N in the complexes with two pyrazole coordinating nitrogen results also in corresponding differences in their spin-spin coupling. The magnitude of spin-spin interaction ^{1}J(Ru-Cl) is lower in monodentate compared to bidentate complexes and even much lower upon their hydrolysis. Also, there is significant increase in the magnitude of ^{1}J(C4-H) and ^{1}J(N-H) upon hydrolysis. While the coupling of ^{1}J(N-N) decreases slightly upon hydrolysis (except for its increased hydrolysed complex **2b** compared to its nonhydrolysed form **2a**). The most significant Ramsey term that contributes significantly in most of the spin-spin interactions is FC except for the Ru-Cl and N-N* which are predominantly defined by the contribution from the PSO. Also, it is only in ^{1}J(Ru-Cl) that the contribution from SD was found higher than the FC contribution. Even though in many of the interactions of interest the PSO contribution is significant than DSO and SD values yet it has poorer correlation with the trend of changes in the spin-spin interaction than DSO and SD.

Conflict of Interests

The authors declare that there is no conflict of interests regarding the publication of this paper.

Acknowledgments

The authors gracefully acknowledge the financial support of Govan Mbeki Research and Development Centre, University of Fort Hare, South Africa. The CHPC in Republic of South Africa is gracefully acknowledged for providing the computing facilities and some of the software used for the computation.

References

[1] M. W. Stanford, F. R. Knight, K. S. Athukorala Arachchige et al., "Probing interactions through space using spin-spin coupling," *Dalton Transactions*, vol. 43, no. 17, pp. 6548–6560, 2014.

[2] L. Ernst and P. Sakhaii, "Investigation of ^{19}F–^{19}F spin–spin coupling in 1-(*x*-fluorophenyl)-8-(*y*-fluorophenyl)naphthalenes (*x*, *y* = 2, 3, 4)," *Magnetic Resonance in Chemistry*, vol. 38, no. 7, pp. 559–565, 2000.

[3] F. A. Perras and D. L. Bryce, "Theoretical study of homonuclear *J* coupling between quadrupolar spins: single-crystal, DOR, and *J*-resolved NMR," *Journal of Magnetic Resonance*, vol. 242, pp. 23–32, 2014.

[4] J. E. Del Bene, J. Elguero, and I. Alkorta, "Computed spin-spin coupling constants ($^{1}J_{X-Y}$) in molecules H_mX–YH_n for X and Y = ^{13}C, ^{15}N, and ^{31}P: comparisons with experiment and insights into the signs of $^{1}J_{X-Y}$," *The Journal of Physical Chemistry A*, vol. 108, no. 16, pp. 3662–3667, 2004.

[5] J. E. Del Bene, I. Alkorta, and J. Elguero, "A systematic comparison of second-order polarization propagator approximation and equation-of-motion coupled cluster singles and doubles C–C, C–N, N–N, C–H, and N–H spin–spin coupling constants," *Journal of Physical Chemistry A*, vol. 113, no. 45, pp. 12411–12420, 2009.

[6] J. Autschbach, A. M. Kantola, and J. Jokisaari, "NMR measurements and density functional calculations of the ^{199}Hg–^{13}C spin-spin coupling tensor in methylmercury halides," *The Journal of Physical Chemistry A*, vol. 111, no. 24, pp. 5343–5348, 2007.

[7] J. E. Del Bene, I. Alkorta, and J. Elguero, "Probing ^{1}J(C-F) and ^{n}J(F-F) spin-spin coupling constants for fluoroazines: an Ab initio theoretical investigation," *The Journal of Physical Chemistry A*, vol. 114, no. 7, pp. 2637–2643, 2010.

[8] D. Cremer and J. Grafenstein, "Calculation and analysis of NMR spin-spin coupling constants," *Physical Chemistry Chemical Physics*, vol. 9, no. 22, pp. 2791–2816, 2007.

[9] G. Gasser, I. Ott, and N. Metzler-Nolte, "Organometallic anticancer compounds," *Journal of Medicinal Chemistry*, vol. 54, no. 1, pp. 3–25, 2011.

[10] M. Hanif, H. Henke, S. M. Meier et al., "Is the reactivity of M(II)-arene complexes of 3-hydroxy-2(1*H*)-pyridones to biomolecules the anticancer activity determining parameteŕ," *Inorganic Chemistry*, vol. 49, no. 17, pp. 7953–7963, 2010.

[11] A. E. Egger, C. G. Hartinger, A. K. Renfrew, and P. J. Dyson, "Metabolization of [Ru(η^6-$C_6H_5CF_3$)(pta)Cl_2]: a cytotoxic RAPTA-type complex with a strongly electron withdrawing arene ligand," *Journal of Biological Inorganic Chemistry*, vol. 15, no. 6, pp. 919–927, 2010.

[12] F. Wang, A. Habtemariam, E. P. L. van der Geer et al., "Controlling ligand substitution reactions of organometallic complexes: tuning cancer cell cytotoxicity," *Proceedings of the National Academy of Sciences of the United States of America*, vol. 102, no. 51, pp. 18269–18274, 2005.

[13] M. J. Frisch, G. W. Trucks, H. B. Schlegel et al., *Gaussian 09, Revision D.01*, Gaussian Inc, Wallingford, Conn, USA, 2009.

[14] J. P. Perdew, K. Burke, and M. Ernzerhof, "Generalized gradient approximation made simple," *Physical Review Letters*, vol. 77, no. 18, pp. 3865–3868, 1996.

[15] J. P. Perdew, K. Burke, and M. Ernzerhof, "Generalized gradient approximation made simple [Phys. Rev. Lett. 77, 3865 (1996)]," *Physical Review Letters*, vol. 78, no. 7, p. 1396, 1997.

[16] R. Ditchfield, W. J. Hehre, and J. A. Pople, "Self-consistent molecular-orbital methods. IX. An extended gaussian-type basis for molecular-orbital studies of organic molecules," *The Journal of Chemical Physics*, vol. 54, pp. 724–728, 1971.

[17] W. J. Hehre, K. Ditchfield, and J. A. Pople, "Self-consistent molecular orbital methods. XII. Further extensions of gaussian-type basis sets for use in molecular orbital studies of organic molecules," *The Journal of Chemical Physics*, vol. 56, no. 5, pp. 2257–2261, 1972.

[18] M. S. Gordon, "The isomers of silacyclopropane," *Chemical Physics Letters*, vol. 76, no. 1, pp. 163–168, 1980.

[19] W. J. Stevens, M. Krauss, H. Basch, and P. G. Jasien, "Relativistic compact effective potentials and efficient, shared-exponent basis sets for the third-, fourth-, and fifth-row atoms," *Canadian Journal of Chemistry*, vol. 70, no. 2, pp. 612–630, 1992.

[20] D. J. Feller, "The role of databases in support of computational chemistry calculations," *Journal of Computational Chemistry*, vol. 17, no. 13, pp. 1571–1586, 1996.

[21] K. L. Schuchardt, B. T. Didier, T. Elsethagen et al., "Basis set exchange: a community database for computational sciences," *Journal of Chemical Information and Modeling*, vol. 47, no. 3, pp. 1045–1052, 2007.

[22] R. Marchal, P. Carbonnière, D. Begue, and C. Pouchan, "Structural and vibrational determination of small gallium—arsenide clusters from CCSD(T) and DFT calculations," *Chemical Physics Letters*, vol. 453, no. 1–3, pp. 49–54, 2008.

[23] R. Marchal, P. Carbonnière, and C. Pouchan, "Structural and vibrational properties prediction of Sn_n Te_n clusters (n = 2–8) using the GSAM approach," *Computational and Theoretical Chemistry*, vol. 990, pp. 100–105, 2012.

[24] H. Kusama, T. Funaki, and K. Sayama, "Theoretical study of cyclometalated Ru(II) dyes: implications on the open-circuit voltage of dye-sensitized solar cells," *Journal of Photochemistry and Photobiology A: Chemistry*, vol. 272, pp. 80–89, 2013.

[25] Z.-Y. Li, H.-L. Wang, T.-J. He, F.-C. Liu, and D.-M. Chen, "Theoretical study on the structure and UV-visible spectrum of pyridine-chloranil charge-transfer complex," *Journal of Molecular Structure: THEOCHEM*, vol. 778, no. 1–3, pp. 69–76, 2006.

[26] C. Adamo and V. Barone, "Exchange functionals with improved long-range behavior and adiabatic connection methods without adjustable parameters: the *m*PW and *m*PW1PW models," *The Journal of Chemical Physics*, vol. 108, no. 2, pp. 664–675, 1998.

[27] L. Pejov, M. Solimannejad, and V. Stefov, "The π-type hydrogen bond with triple C–C bond acting as a proton-acceptor. A gradient-corrected hybrid HF-DFT and MP2 study of the phenol–acetylene dimer in the neutral S_0 ground state," *Chemical Physics*, vol. 323, no. 2-3, pp. 259–270, 2006.

[28] H. Kusama and K. Sayama, "Theoretical study on the intermolecular interactions of black dye dimers and black dye-deoxycholic acid complexes in dye-sensitized solar cells," *Journal of Physical Chemistry C*, vol. 116, no. 45, pp. 23906–23914, 2012.

[29] T. Helgaker, M. Watson, and N. C. Handy, "Analytical calculation of nuclear magnetic resonance indirect spin-spin coupling constants at the generalized gradient approximation and hybrid levels of density-functional theory," *Journal of Chemical Physics*, vol. 113, no. 21, pp. 9402–9409, 2000.

[30] V. Sychrovský, J. Gräfenstein, and D. Cremer, "Nuclear magnetic resonance spin-spin coupling constants from coupled perturbed density functional theory," *The Journal of Chemical Physics*, vol. 113, no. 9, pp. 3530–3547, 2000.

[31] A. D. Becke, "Density-functional thermochemistry. III. The role of exact exchange," *The Journal of Chemical Physics*, vol. 98, no. 7, pp. 5648–5652, 1993.

[32] N. Godbout, D. R. Salahub, J. Andzelm, and E. Wimmer, "Optimization of Gaussian-type basis sets for local spin density functional calculations. Part I. Boron through neon, optimization technique and validation," *Canadian Journal of Chemistry*, vol. 70, no. 2, pp. 560–571, 1992.

[33] C. Sosa, J. Andzelm, B. C. Elkin, E. Wimmer, K. D. Dobbs, and D. A. Dixon, "A local density functional study of the structure and vibrational frequencies of molecular transition-metal compounds," *Journal of Physical Chemistry*, vol. 96, no. 16, pp. 6630–6636, 1992.

[34] D. Sanz, R. M. Claramunt, I. Alkorta, G. Sánchez-Sanz, and J. Elguero, "The structure of glibenclamide in the solid state," *Magnetic Resonance in Chemistry*, vol. 50, no. 3, pp. 246–255, 2012.

[35] S. Komiya and M. Hurano, "Group 8 (Fe, Ru, Os) metal compounds," in *Synthesis of Organometallic Compounds: A Practical Guide*, S. Komiya, Ed., pp. 159–203, John Wiley & Sons, London, UK, 1997.

[36] A. Casini, C. Gabbiani, F. Sorrentino et al., "Emerging protein targets for anticancer metallodrugs: inhibition of thioredoxin reductase and cathepsin B by antitumor ruthenium(II)-arene compounds," *Journal of Medicinal Chemistry*, vol. 51, no. 21, pp. 6773–6781, 2008.

[37] A. K. Renfrew, A. D. Phillips, E. Tapavicza, R. Scopelliti, U. Rothlisberger, and P. J. Dyson, "Tuning the efficacy of ruthenium(II)-arene (RAPTA) antitumor compounds with fluorinated arene ligands," *Organometallics*, vol. 28, no. 17, pp. 5061–5071, 2009.

[38] X. Shang, T. F. S. Silva, L. M. D. R. S. Martins et al., "Synthesis, characterization, electrochemical behavior and *in vitro* protein tyrosine kinase inhibitory activity of the cymene-halogenobenzohydroxamato [Ru(η^6-cymene)(bha)Cl] complexes," *Journal of Organometallic Chemistry*, vol. 730, pp. 137–143, 2013.

[39] D. Belli Dell'Amico, F. Calderazzo, L. Labella, F. Marchetti, and E. Sbrana, "Organometallic complexes of ruthenium(II) with *N*,*N*-dialkylcarbamato as the supporting ligand," *Journal of Organometallic Chemistry*, vol. 651, no. 1-2, pp. 52–59, 2002.

[40] M. Melchart, A. Habtemariam, S. Parsons, S. A. Moggach, and P. J. Sadler, "Ruthenium(II) arene complexes containing four- and five-membered monoanionic O,*O*-chelate rings," *Inorganica Chimica Acta*, vol. 359, no. 9, pp. 3020–3028, 2006.

[41] F. Caruso, M. Rossi, A. Benson et al., "Ruthenium-arene complexes of curcumin: X-ray and density functional theory structure, synthesis, and spectroscopic characterization, in vitro antitumor activity, and DNA docking studies of (*p*-cymene)Ru(curcuminato)chloro," *Journal of Medicinal Chemistry*, vol. 55, no. 3, pp. 1072–1081, 2012.

[42] C. A. Vock, C. Scolaro, A. D. Phillips, R. Scopelliti, G. Sava, and P. J. Dyson, "Synthesis, characterization, and in vitro evaluation of novel ruthenium(II) η^6-arene imidazole complexes," *Journal of Medicinal Chemistry*, vol. 49, no. 18, pp. 5552–5561, 2006.

[43] J. Canivet, L. Karmazin-Brelot, and G. Süss-Fink, "Cationic arene ruthenium complexes containing chelating 1,10-phenanthroline ligands," *Journal of Organometallic Chemistry*, vol. 690, no. 13, pp. 3202–3211, 2005.

[44] S. Betanzos-Lara, L. Salassa, A. Habtemariam et al., "Photoactivatable organometallic pyridyl ruthenium(II) arene complexes," *Organometallics*, vol. 31, no. 9, pp. 3466–3479, 2012.